

(γ, n) Cross Sections of Nuclides near Neutron Number 50*

PAUL F. YERGIN† AND BURTON P. FABRICAND
University of Pennsylvania, Philadelphia, Pennsylvania
 (Received August 30, 1956)

Measurement of the (γ, n) cross sections of the nuclides Sr^{86} , Sr^{87} , Sr^{88} , Y^{89} , Zr^{92} , together with earlier measurements for the nuclides Zr^{90} , Zr^{91} , and Nb^{93} , show a pronounced narrowing of the giant dipole resonances in the region of neutron number 50, the narrowest resonances being those for the 50-neutron nuclides. Possible confusion of the interpretation of the data due to $(\gamma, 2n)$ and (γ, pn) processes is shown to be inadequate to explain the observed effects, and the narrowing is concluded to be real, in agreement with the prediction of the single-particle model of Wilkinson. The changes in widths are observed to occur entirely on the high-energy sides of the curves, the low-energy sides being remarkably similar for all 8 nuclides. A regularity in the behavior of the peak values of the cross sections is also observed. The (γ, n) threshold of Sr^{86} is observed to be at about 11.5 Mev, in agreement with other reaction data, but in disagreement with an earlier tentative assignment based on neutron yield measurements on natural Sr.

INTRODUCTION

THE considerable regularities observed in the characteristics of the giant dipole resonance in photonuclear reactions suggest similar considerable regularities in the characteristics of the highly excited (12 to 22 Mev) states involved in these reactions, as well as of the ground states of nuclei. Both the collective and single-particle models of the nucleus have been able to give qualitative descriptions of the photonuclear processes, despite the seemingly opposite nature of their assumptions.¹ The collective model gives about the right variation of the location of the peak of the resonance with mass number, but does not give any other detailed features, except for the suggestion that the widths of the resonances are correlated with the nuclear quadrupole moments² and there are some substantial exceptions to this. The single-particle model makes more detailed predictions,³ such as the occurrence of "steps" in the locations of the peaks whenever a shell is closed, which is not well supported experimentally, the decrease with decreasing mass number of the fraction of the dipole sum rule which is included in the giant resonance, which is observed, and the excess emission of protons from the very heavy nuclei, which is also observed. A further qualitative prediction of the single-particle model is that the resonances should be broadened when partly filled shells are present in the nucleus, as compared to the simpler case when the nucleus consists entirely of closed shells. It has been observed in a number of

cases^{4,5} that the resonances for "magic number" nuclei are substantially narrower than for other nuclei. The present experiment was designed to test this point rather critically, by examining a number of nuclei with 50 neutrons, and to establish whether the narrowing in the region of a magic number of neutrons is gradual or abrupt by examining nuclei with slightly more or less than 50 neutrons.

EXPERIMENT

Since Zr^{90} , Zr^{91} , and Nb^{93} , with 50, 51, and 52 neutrons respectively, had been investigated earlier we chose the nuclides Sr^{86} , Sr^{87} , Sr^{88} , Y^{89} , and Zr^{92} , with 48, 49, 50, 50, and 52 neutrons, respectively, for the present experiment. (There are Rb, Mo, and Kr isotopes in this neutron number region also, but they were not available in the required quantities.⁶) The Sr and Zr were obtained on loan from Oak Ridge National Laboratory, while the Y was purchased commercially.

The isotopic compositions of the samples is shown in Table I, which includes information for the Zr^{90} and Zr^{91} samples reported earlier because the data for all three Zr samples was treated anew in computing the cross sections for individual isotopes, taking into account the composition of each sample. Yttrium is monoisotopic. The Sr samples were in the form of SrCO_3 , the Y was in the form of Y_2O_3 , and the Zr samples were all in the form of ZrO_2 . The samples were held in a sample holder such that they were entirely within the collimated gamma-ray beam, in essentially the same way as described for Mg^{25} previously.⁵ They were irradiated with the bremsstrahlung gamma rays from the 24-Mev betatron. The neutrons ejected from the nuclei were detected in the large paraffin house neutron detector.⁷ To verify that the energy-insensitive

* Supported in part by the U. S. Air Research and Development Command and the joint program of the Office of Naval Research and the U. S. Atomic Energy Commission.

† Present address: Physics Department, Rensselaer Polytechnic Institute, Troy, New York.

¹ See the survey of this situation by J. Levinger in *Annual Reviews of Nuclear Science* (Annual Reviews, Inc. Stanford, 1954), Vol. 4, p. 13 ff.

² K. Okamoto, *Progr. Theoret. Phys. Japan* **15**, 75 (1956).

³ D. H. Wilkinson, *Proceedings of the Glasgow Conference on Nuclear and Meson Physics 1954* (Pergamon Press, London, 1955), p. 161.

⁴ R. Nathans and J. Halpern, *Phys. Rev.* **93**, 437 (1954).

⁵ R. Nathans and P. F. Yergin, *Phys. Rev.* **98**, 1296 (1955).

⁶ There are published measurements made in other laboratories of the cross sections of some of these and other isotopes in this region of neutron number, but for reasons given in reference 4, we are unwilling to make critical comparisons of data unless it all comes from one laboratory and one set of apparatus.

⁷ Halpern, Mann, and Nathans, *Rev. Sci. Instr.* **23**, 678 (1952)

TABLE I. Isotopic compositions of the Sr and Zr samples. The entries give the atomic percent of each isotope in the sample whose nominal label is given in the first column. In the reduction of the data, Sr⁸⁴ was counted as though it was Sr⁸⁶, and Zr⁹⁴ and Zr⁹⁶ were counted as though they were Zr⁹². The analyses are those supplied by ORNL.

Sample	Sr ⁸⁴	Sr ⁸⁶	Sr ⁸⁷	Sr ⁸⁸
Sr ⁸⁶	0.02	83.44	2.03	14.52
Sr ⁸⁷	...	2.56	42.82	54.63
Sr ⁸⁸	...	0.08	0.29	99.63
Natural Sr	0.56	9.86	7.02	82.56

Sample	Zr ⁹⁰	Zr ⁹¹	Zr ⁹²	Zr ⁹⁴	Zr ⁹⁶
Zr ⁹⁰	98.66	0.77	0.34	0.18	0.04
Zr ⁹¹	12.3	75.1	10.5	1.9	0.2
Zr ⁹²	2.4	2.2	92.7	2.3	0.4

property of the detector had not changed, a trial run was made with a gold target. The yield data were converted to cross-section values and compared with the published curve.⁴ The absolute magnitudes and shapes of the two curves agreed to about 10%, all the way up to 23 Mev.

A substantial reduction of background was obtained by putting an aluminum tube through the beam hole in the neutron house, and evacuating it. The sample holder fitted inside this tube. Further background reduction was accomplished by putting a 1-in. long lead slug, with a hole through it just large enough to pass the gamma-ray beam, at the entrance to the evacuated tube. It appears that this slug "scrapes off" gamma rays which are traveling adjacent to the main beam, not quite parallel to it, and which would otherwise strike the walls of the beam hole inside the neutron house. These stray gamma rays may arise from small angle scatterings in the collimator. The general shielding around the betatron was also considerably improved. The background counting rate was not greater than 3% of the neutron yield at maximum energy (23 Mev), and increased somewhat at lower energies.

The total number of counts recorded, at all energies, for each sample is shown in Table II. Except at points within about 1.5 Mev of threshold at least 10 000, and often 40 000 counts were taken for each point, in at least three, and usually 6 runs at different times. The points were about 0.8 Mev apart in energy. The gamma-ray exposures were measured by a Victoreen 250-roentgen thimble in a cylindrical Lucite block of 3.75 cm radius. The bremsstrahlung tables used in the data reduction were prepared for this monitoring arrangement. The absolute sensitivity of the neutron detector was measured with a Ra-Be neutron source calibrated by the National Bureau of Standards.

CALCULATIONS

In the usual way, we have reduced the experimental yield values to cross-section values by replacing the

TABLE II. The total counts recorded for each sample are shown in column 2. The total mass of the sample is shown in column 3. The area density of the sample in the direction of the gamma-ray beam is shown in column 4. The counts in column 2 do not include the check-point counts taken at 21.12 Mev, which were partly used in the data reduction, and in most cases were one-half to one times as large as the total counts listed.

Sample	Total counts recorded	Mass of sample (g)	Area density (g/cm ²)
Sr ⁸⁶	513 500	1.120	2.429
Sr ⁸⁷	280 000	0.552	1.115
Sr ⁸⁸	384 800	0.817	1.652
Natural Sr	550 800	1.528	3.088
Y ⁸⁹	667 000	1.663	3.361
Zr ⁹⁰	687 000	1.606	2.253
Zr ⁹¹	309 000	0.446	0.626
Zr ⁹²	617 309	1.317	2.661

integral equations

$$Y(E_i) = Q \int_0^{E_i} N'(E_i, k) \sigma'(k) dk, \quad i = 1, 2, 3, \dots, n, \quad (1)$$

where $Y(E_i)$ is the neutron yield per roentgen of irradiation, when the maximum energy of the bremsstrahlung is E_i , $N'(E_i, k)$ is the number of photons at energy k per cm² per unit energy interval per roentgen of irradiation when the maximum energy of the bremsstrahlung is E_i , $\sigma'(k)$ is the cross section for ejection from the nucleus of a neutron by a photon of energy k , and Q is the number of nuclei exposed to the gamma-ray beam; by the equations

$$Y(E_i) = Q \sum_{k=0}^{k=E_i} N(E_i, k) \sigma(k) \quad i = 1, 2, \dots, n, \quad (2)$$

where $N(E_i, k)$ is the number of photons having energies between $k - \Delta k$ and k per cm² per roentgen of irradiation when the maximum energy of the bremsstrahlung is E_i , and $\sigma(k)$ is a certain weighted average of the cross section for neutron ejection from target nuclei by photons in the energy range $k - \Delta k$ to k . (Δk is the interval of the values of k). Penfold⁸ has examined the justification of this replacement, and finds that in cases of the sort dealt with in the present work, the cross-section values obtained by solving these equations are very close to the cross sections which would be obtained in a solution of Eq. (1) for the energies $k - \frac{1}{2}\Delta k$. For this to be true, it is necessary only that the structure of the cross-section curve be broad compared to the interval Δk . We use a 1-Mev bin width in the data reduction, and the narrowest observed curve has a half-width of 4 Mev.

It is well known that in the use of Eq. (2) the increase by a small amount of a single yield value, say at an energy E_0 , will increase the cross section calculated for the point $E_0 - \frac{1}{2}\Delta k$ by a large amount, will decrease the cross section for the point $E_0 + \frac{1}{2}\Delta k$ by a similarly large amount, and will have a smaller effect on higher energy

⁸ A. S. Penfold (private communication).

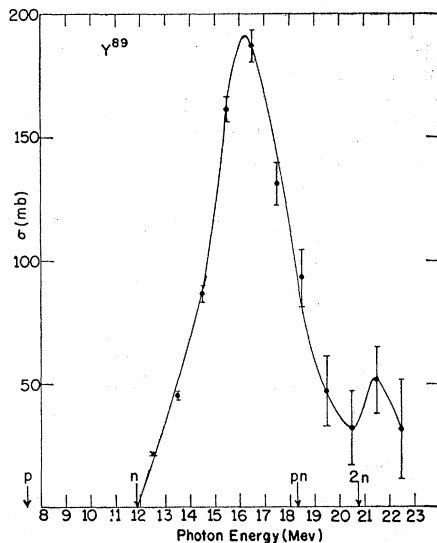


FIG. 1. Cross section for the (γ, n) reaction in Y^{89} , calculated from the yield data, at an intermediate stage of the smoothing process (see text). The vertical lines through the calculated points show the rms uncertainty in the cross-section values, produced by the statistical uncertainty of the recorded counts of the raw yield data. Other sources of errors, and the partial smoothing already done have been ignored in calculating these uncertainties. The arrows along the abscissa indicate the thresholds for emission of the particles indicated by the labels therewith. The units of the ordinate are 10^{-27} cm 2 .

points. Because of the "oscillation" effect produced by small irregularities in the yield curves, it is common practice arbitrarily to smooth the experimental yield curve before performing the calculations⁹ (or to use hindsight to obtain a smoother curve, after a trial calculation has been performed, which is what we have done in the present case).

Despite the apparently arbitrary nature of this procedure, it is possible to assert that the only real violence which may have been done to the experimental data is the smoothing out of real irregularities in the cross-section curve. The smoothing is never allowed to adjust the yield points by an unlikely amount relative to their experimental uncertainties. A direct calculation of the dependence on the yield values of the "integrated cross section", that is, the area under the cross section *vs* energy curve, shows that the uncertainty in this quantity is actually quite small, even though the uncertainties of individual cross-section points are quite large. As an example, Fig. 1 shows the cross section calculated for Y^{89} , at an intermediate stage in the data smoothing procedure. The uncertainty indicated with each point is that due to the statistical uncertainty in numbers of counts at the yield points. The "oscillation" effect described above indicates a high degree of correlation between adjacent points, however, and the uncertainty in the area under the curve of Fig. 1 is only 1.6%. We can conclude that the calculated

⁹ L. Katz and A. G. W. Cameron, Can. J. Phys. **29**, 518 (1951).

cross-section curves do represent the true cross-section curves, with the exception mentioned above, that all fine structure is eliminated. With this in mind we have eliminated from our final curves all details, such as the rise in cross section at the high-energy end of the scale shown in Fig. 1. The final curve for Y^{89} (Fig. 4) shows the result of doing this. In all cases, the smoothing was only important on the high-energy side of the resonance curves. As a check, the yield curves were "reconstituted" by using Eq. (2), and were found to agree within experimental uncertainties with the original data.

RESULTS

The cross-section curves for Sr^{86} , Sr^{87} , and Sr^{88} with 48, 49, and 50 neutrons, respectively, are shown in Fig. 2. The principal features of interest are that the location of the peak is very nearly the same for all three, the width at half-maximum height is greater for the nonmagic Sr^{86} and Sr^{87} than it is for Sr^{88} , and the peak cross sections are smaller for Sr^{86} and Sr^{87} than for Sr^{88} . As a check on the data for the strontium isotopes, the cross section for natural strontium was measured. The cross section computed by taking the appropriate proportions of the three isotopes Sr^{86} , Sr^{87} and Sr^{88} is compared with the measured cross section in Fig. 3. (The points shown in Fig. 3 have not been smoothed to the same extent as the result shown in Figs. 2, 4, and 5. The only smoothing done for these points is that involved in graphical interpolation of the

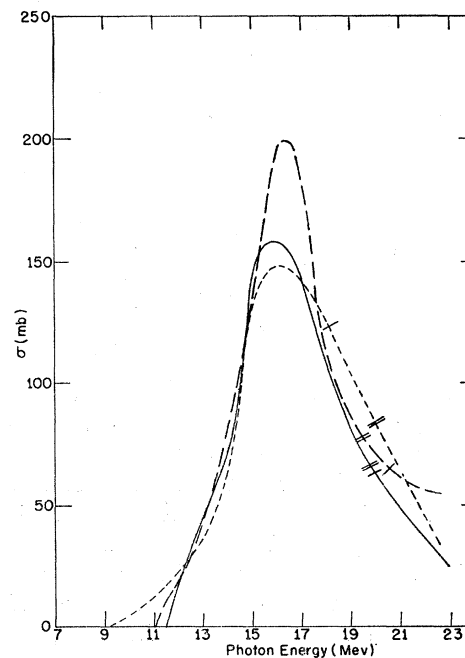


FIG. 2. Cross sections for the (γ, n) reactions in strontium isotopes. Full curve Sr^{86} , short dashes Sr^{87} , long dashes Sr^{88} . The single and double slash marks on each curve represent the locations of the (γ, pn) and $(\gamma, 2n)$ thresholds, respectively. The units of the ordinate are 10^{-27} cm 2 .

yields at Mev points between the measured yield points, which were not at even Mev values in general. The comparison is therefore a more critical one than if the smoothing had all been done first.) In the case of Zr such a comparison would not have been useful because of the large natural abundances of Zr^{94} and Zr^{96} , for which cross-section data are not available, so we did not measure the cross section of natural Zr.

The cross-section curves for the three magic-number nuclei Sr^{88} , Y^{89} , and Zr^{90} are shown in Fig. 4. The close similarities of the three curves is remarkable, as is their uniform narrowness.

The cross-section curves for Zr^{90} , Zr^{91} and Zr^{92} , with 50, 51, and 52 neutrons, respectively, are shown in Fig. 5. The data for the Zr^{90} and Zr^{91} samples have been combined with the Zr^{92} data in a new calculation of the isotope cross-section curves, and there are small differences from the previously published curves,⁵ including correction of an arithmetic error which makes the Zr^{90} absolute cross section about 10% higher. The interesting features are that the nonmagic nuclei again have wider curves than the magic number nucleus Zr^{90} , and the curves all have the same peak height. The parameters of the cross-section curves for all the cases measured in this laboratory from mass number 75 to 103 are given in Table III.

The energy region from 12.5 to 15.5 Mev is shown expanded in Fig. 6. The points shown are the cross-section values calculated for the 1-Mev bins for each of the 8 nuclides having from 48 to 52 neutrons which have been measured in this laboratory. The points are connected by straight lines for visual purposes only.

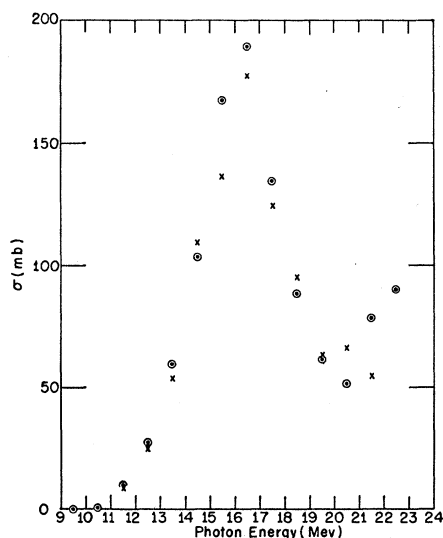


FIG. 3. Comparison of unsmoothed cross-section calculations for natural strontium sample with the values obtained by combining in proper proportion the cross sections for the isotopes Sr^{86} , Sr^{87} , and Sr^{88} . The circles show the results of the direct measurement, and the crosses show the isotopic combination values. See text for remarks about smoothing. The units of the ordinate are 10^{-27} cm².

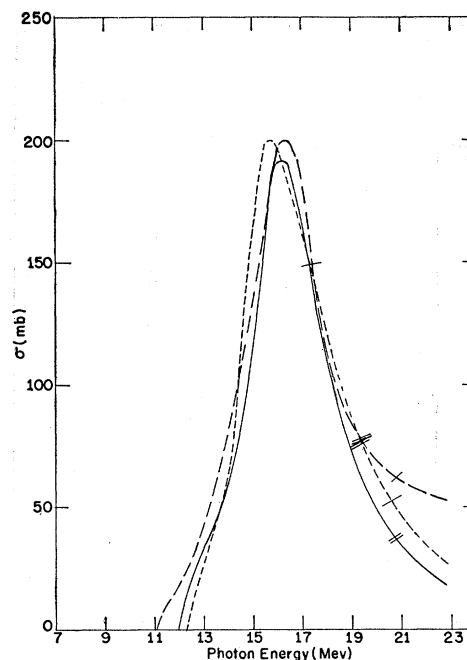


FIG. 4. Cross sections for the (γ, n) reactions in 50-neutron nuclides. Long dashes Sr^{88} , full curve Y^{89} , short dashes Zr^{90} . The single and double slash marks on each curve represent the locations of the (γ, pn) and $(\gamma, 2n)$ thresholds, respectively. The units of the ordinate are 10^{-27} cm².

The remarkable feature of this graph is the close agreement of all 8 curves in this energy region, which covers the low-energy half of the giant resonance. At 15 Mev the spread of the cross-section values is only 3 times the statistical uncertainties in the values. The locations of the half-height points on the curves range from 14 to 14.6 Mev, which is a narrower range than that of the location of the peaks of the curves for these nuclei.

The (γ, n) threshold of Sr^{86} was reported tentatively by Sher, Halpern, and Mann¹⁰ at 9.5 Mev. It has been pointed^{11,12} out that this value is unlikely, in view of other reaction data and mass data, which suggest a value near the threshold of Sr^{88} at 11 Mev. The calculations indicate most likely values of the Sr^{86} threshold to be 11.0 or 11.5 Mev. We did not make a careful measurement of the Sr^{86} threshold, but our data indicate that it is between 10.5 and 12.0 Mev, with the most likely value near 11.5 Mev, in agreement with these suggestions.

DISCUSSION

The onset of $(\gamma, 2n)$ processes can make the resonance curves appear wider in the present experiments, where neutrons are detected, since the neutron multiplicity will be interpreted as a larger cross section. [In experiments where the residual activity is measured, the

¹⁰ Sher, Halpern, and Mann, Phys. Rev. 84, 387 (1951).

¹¹ A. H. Wapstra, Physica 21, 385 (1955).

¹² V. A. Kravtsov, Bull. Acad. Sci. U.S.S.R. 19, 338 (1955).

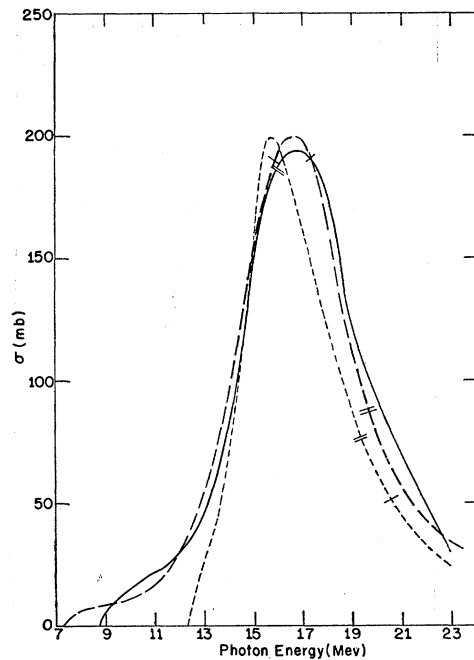


FIG. 5. Cross sections for the (γ, n) reactions in zirconium isotopes. Short dashes Zr^{90} , long dashes Zr^{91} , full curve Zr^{92} . The previously published Zr^{90} and Zr^{91} results have been recomputed, taking into account the present Zr^{92} measurements. The single and double slash marks on each curve represent the locations of the (γ, pn) and $(\gamma, 2n)$ thresholds respectively. The units of the ordinate are 10^{-27} cm².

$(\gamma, 2n)$ competition would make the curves appear narrower.] The onset of (γ, pn) processes can have a similar effect, since at energies where only (γ, p) or (γ, n) can occur we see only the (γ, n) events, while at energies where (γ, pn) can occur this process will compete with both (γ, n) and (γ, p) , and will always be counted by us as (γ, n) , which means that in effect some of the (γ, p) cross section is added to the neutron emission cross section above the (γ, pn) threshold. In fact, at energies far enough above this threshold, one would expect that most of the events in which a proton was emitted would be accompanied by neutron emission. This has in fact been observed¹³ in the light elements F and N.

These processes certainly do affect the shapes of the observed curves. There are, however, some clear-cut cases where the measured half-widths cannot have been thus affected. The three magic nuclei Sr^{88} , Y^{89} , and Zr^{90} all have (γ, pn) and $(\gamma, 2n)$ thresholds,¹⁴ indicated on the curves of Figs. 2, 4, and 5 by single and double slash marks, respectively, too high in energy to affect the half-widths seen. The increased half-widths of the non-magic-number nuclei Sr^{86} and Sr^{87} , as compared to that of Sr^{88} , cannot be ascribed to these processes,

¹³ Ferguson, Halpern, Nathans, and Yergin, Phys. Rev. **95**, 776 (1954).

¹⁴ We have used throughout threshold values derived from the compilation of reference 9.

either, as indicated by their thresholds, shown on Fig. 2. [Even the (γ, pn) threshold of Sr^{87} cannot have any significant effect, since appreciable proton emission cannot occur for several Mev above the threshold.] In similar fashion, Fig. 5 shows that the increased width of the Zr^{91} curve over that of Zr^{90} is not due to the $(\gamma, 2n)$ process.

The smoothing which is done in the calculations, as described above, cannot have produced the differences in half-widths, because of the restrictions imposed by the requirement that the integrated cross sections, which are well determined by the data, stay within bounds. In a sense, it might be more direct to specify something like the energy interval, symmetric around the peak, in which the integrated cross section divided by the interval is equal to say, three-quarters of the peak cross section. This would in fact not produce relative widths very different from those given by the half-height energy interval. The only likely effect of the smoothing is that the narrower peaks may appear to be wider than they really should be.

The close agreement of all eight curves in the region of the low-energy slope of the resonances, despite their considerable differences on the high-energy side, suggests that this part of the curve is only very slightly sensitive to details of nuclear structure. It has been suggested that the half-height point on the low-energy side of the curve is a more regular parameter than the location of the peak. Experimentally this point is easier to locate than the peak of the curve, because the cross-section points are more accurately determined in this region, and the curve is steeper. Any error in the peak cross section caused by the bin size not being small enough will not shift the half-height point much, because of the steepness of the curve. Since the present work shows on the other hand, that the high-energy side of the resonance does depend strongly on details of nuclear structure, the location in energy of the peak will very likely also be affected.

TABLE III. Parameters of giant-resonance cross-section curves for (γ, n) reactions in nuclei near 50 neutrons. Nuclides $^{33}As^{75}$, $^{41}Nb^{93}$, and $^{45}Rh^{103}$ from reference 4, $^{40}Zr^{90}$ and $^{40}Zr^{91}$ from reference 5 recomputed in present work. Neutron number is shown in column 2, location of peak cross-section value in column 3, peak cross-section value in column 4, half-height width of curve in column 5, and area under curve from threshold to 23 Mev in column 6.

Nuclide	N	E_m (Mev)	σ_m (millibarns)	Γ (Mev)	$\int_0^{23} \sigma dE$ (Mev-barns)
$^{33}As^{75}$	42	17.3	90.3	9.0	0.80
$^{38}Sr^{86}$	48	15.9	160	5.0	0.92
$^{38}Sr^{87}$	49	15.8	146	5.3	1.00
$^{38}Sr^{88}$	50	16.3	201	4.0	1.05
$^{39}Y^{89}$	50	16.3	191	3.8	0.87
$^{40}Zr^{90}$	50	15.8	199	4.3	0.98
$^{40}Zr^{91}$	51	16.5	200	5.0	1.22
$^{40}Zr^{92}$	52	16.9	193	5.5	1.24
$^{41}Nb^{93}$	52	17.0	195	6.8	1.46
$^{45}Rh^{103}$	58	16.5	205	8.9	1.94

Santos *et al.*¹⁵ suggest that if shell-structure effects are to be observed in the widths of the giant resonances, one ought to define a width parameter which would not be affected by the extraneous processes $(\gamma, 2n)$, etc. To do this they have used the interval between the peak energy and the extrapolated intercept, with zero cross section, of the line joining the peak of the curve with the low-energy half-height point on the curve. They then find no significant correlation with shell structure. Our observations show why this is so. The low-energy side of the curve is indeed *not* correlated with the shell structure. It is just the difficult-to-investigate high-energy side of the curve which shows the strong shell-structure correlations. The same investigators then suggest that the interval between the (γ, n) threshold and the low-energy half-height point of the giant resonance shows a strong shell-structure effect, and show that this is indeed so. This is not surprising, since the (γ, n) thresholds themselves show a strong shell-structure effect, and it has not been shown that the correlation remains if the part due to the absolute threshold values is removed. Our present work, covering nuclides with widely different (γ, n) thresholds, shows clearly that the absolute location of this half-height point is very little dependent on details of structure or thresholds.

CONCLUSIONS

The photoneutron cross-section curves for the nuclides measured in the neighborhood of 50-neutron nuclides show regularities of the following kinds, which are not due to extraneous effects such as data processing, or competing processes interfering: (1) The giant resonances are much narrower than for nuclides not so close to the neutron number 50, and the 50-neutron nuclides have the narrowest resonances. (2) The low-energy sides of the resonances are remarkably similar for eight nuclides close to neutron number 50, both in absolute cross-section values and in the location of the half-height points. (3) A corollary of the previous points is that the high-energy sides of the resonances vary considerably among these eight nuclides. (4) The

¹⁵ M. D. de Souza Santos *et al.*, *Anais acad. brasil. cienc.* **27**, 437 (1955).

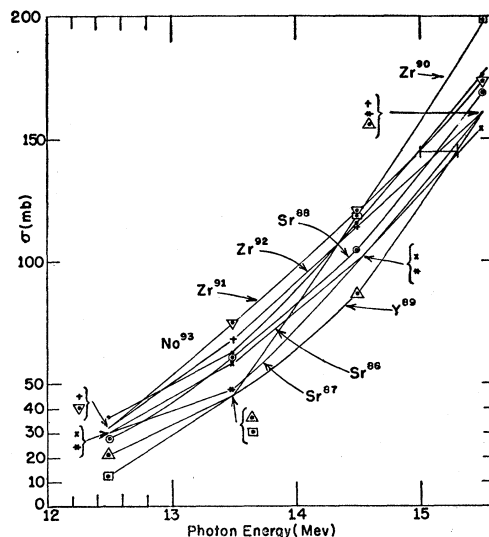


FIG. 6. Cross sections for the (γ, n) reactions in Sr^{86} , Sr^{87} , Sr^{88} , Y^{89} , Zr^{90} , Zr^{91} , Zr^{92} , and Nb^{93} , in the energy region 12.5 to 15.5 Mev. The calculated points for 1-Mev bin widths are plotted at the centers of the bins, and are connected by straight lines, not smoothed curves.

peak heights of the resonance curves are all almost exactly the same (unless perhaps the narrowest curves have been broadened, hence lowered, by the finite bin-width used) except for the two nuclides of the group, Sr^{86} and Sr^{87} , in which the neutron shell is not yet closed, and which have peaks significantly lower than the others.

ACKNOWLEDGMENTS

The work has benefitted from discussions with and support from Dr. J. Halpern. Our confidence in the validity of the data-reduction procedure has been helped by conversation with Dr. A. S. Penfold. We are glad to acknowledge the suggestion by Dr. E. V. Weinstock that the beam hole in the neutron-detecting house be evacuated to reduce the background. The Sr and Zr samples were borrowed from the Stable Isotope Research and Production Division of the Oak Ridge National Laboratory, Dr. C. P. Keim, Director.